JACS
JOURNAL OF THE AMERICAN CHEMICAL SOCIETY

Communication

pubs.acs.org/JACS

A Synthetic Replicator Drives a Propagating Reaction–Diffusion Front

Ilaria Bottero, Jürgen Huck, Tamara Kosikova, and Douglas Philp*

School of Chemistry and EaStCHEM, University of St Andrews, North Haugh, St Andrews, Fife KY16 9ST, U.K.

Supporting Information

ABSTRACT: A simple synthetic autocatalytic replicator is capable of establishing and driving the propagation of a reaction–diffusion front within a 50 μL syringe. This replicator templates its own synthesis through a 1,3-dipolar cycloaddition reaction between a nitrone component, equipped with a 9-ethynylanthracene optical tag, and a maleimide. Kinetic studies using NMR and UV–vis spectroscopies confirm that the replicator forms efficiently and with high diastereoselectivity, and this replication process brings about a dramatic change in optical properties of the sample—a change in the color of the fluorescence in the sample from yellow to blue. The addition of a small amount of the preformed replicator at a specific location within a microsyringe, filled with the reaction building blocks, results in the initiation and propagation of a reaction–diffusion front. The realization of a replicator capable of initiating a reaction–diffusion front provides a platform for the examination of interconnected replicating networks under out-of-equilibrium conditions involving diffusion processes.

The spontaneous generation of stationary patterns and propagating fronts in chemical systems[1] has intrigued scientists for generations. Such phenomena are ubiquitous in nature,[2] and the physical processes behind their appearance and stability have been studied extensively[3] and are now relatively well understood. Propagating reaction–diffusion fronts have received significant attention in this respect. Frequently, one or more oscillatory or autocatalytic processes are found at the core of these systems. Front generation is initiated when an autocatalyst is added at a discrete location in an expanse of reactant, initially at uniform concentration, and the ensuing reaction generates wave fronts, which propagate outward from the initial reaction zone. In almost all[4] of the examples reported to date, the autocatalysis is based on inorganic chemistry, although, more recently, a small number of examples based on RNA[5] and DNA[6] have been described. Self-replication[7] represents a niche of autocatalytic behavior in which a structurally complex template is capable of recognizing the building blocks necessary for its own formation and catalyzing their reaction to form an exact copy of itself. We, and others, have described the use of such systems in instructable networks,[8] as tools for dynamic systemic resolution,[9] and in the construction[10] of mechanically interlocked molecules. Although all of these systems display the nonlinear kinetic characteristics of autocatalytic systems to a greater or lesser extent, in general, they have been studied under well-stirred batch reactor conditions. The consequence of this reaction format places a fundamental limit on the level of complexity and emergence that can be generated by such systems. In order to create diverse emergent behavior, there is a need to study self-replicating systems under out-of-equilibrium conditions, and propagating reaction–diffusion fronts could provide an ideal vehicle for such studies. Here, we report the design and implementation of a molecular replicating system capable of generating and sustaining a propagating reaction–diffusion front.

Previously, we described[11] an efficient synthetic replicator based on the general design shown in Figure 1a. Reaction of nitrone **1a** with maleimide **2** in $CDCl_3$ at −10 °C results in the rapid, autocatalytic formation of the cycloadduct **3a**. Cycloadduct **3a** is a very efficient template for its own formation—it is capable of accelerating the reaction between **1a** and **2** up to 125× through a ternary complex [**1a**·**2**·**3a**], and the structure of this complex ensures that only the *trans* diastereoisomer of **3a** is formed during this process. Conventionally, we have monitored the kinetics of replication processes by NMR spectroscopy. In a reaction–diffusion format, this reaction requires an alternative method to monitor the progress[12] of the reaction. Ideally, we desired an optical signature of replication. Therefore, we designed nitrone **1b**, bearing a 9-ethynylanthracene tag. RM1 calculations (Figure 1b) indicated that this nitrone, in partnership with maleimide **2**, was capable of furnishing template **3b** through a ternary complex, [**1b**·**2**·**3b**]. This complex should permit the formation of only the *trans* diastereoisomer of **3b**. TD-DFT calculations (see Supporting Information) indicated that a significant change in the 350–400 nm region of the UV–vis spectrum could be expected on conversion of nitrone **1b** to cycloadduct **3b** as a result of the presence of the 9-ethynylanthracene unit. We synthesized nitrone **1b** using standard methods; this compound forms yellow-colored solutions in $CDCl_3$, which exhibit an intense yellow fluorescence (Figure 1a). Pleasingly, the conversion of **1b** into **3b** resulted in a very significant color change—the yellow fluorescence of **1b** was replaced (Figure 1a) by the blue fluorescence of **3b**.

Next, we conducted a series of kinetic experiments involving the reaction of **1b** and **2** in $CDCl_3$ at 0 and 20 °C, monitoring the production of cycloadduct **3b** by 500 MHz ^{1}H NMR spectroscopy. The results of these experiments and subsequent fitting of the experimental data at 20 °C to the appropriate

Received: April 1, 2016

DOI: 10.1021/jacs.6b03372
J. Am. Chem. Soc. XXXX, XXX, XXX–XXX

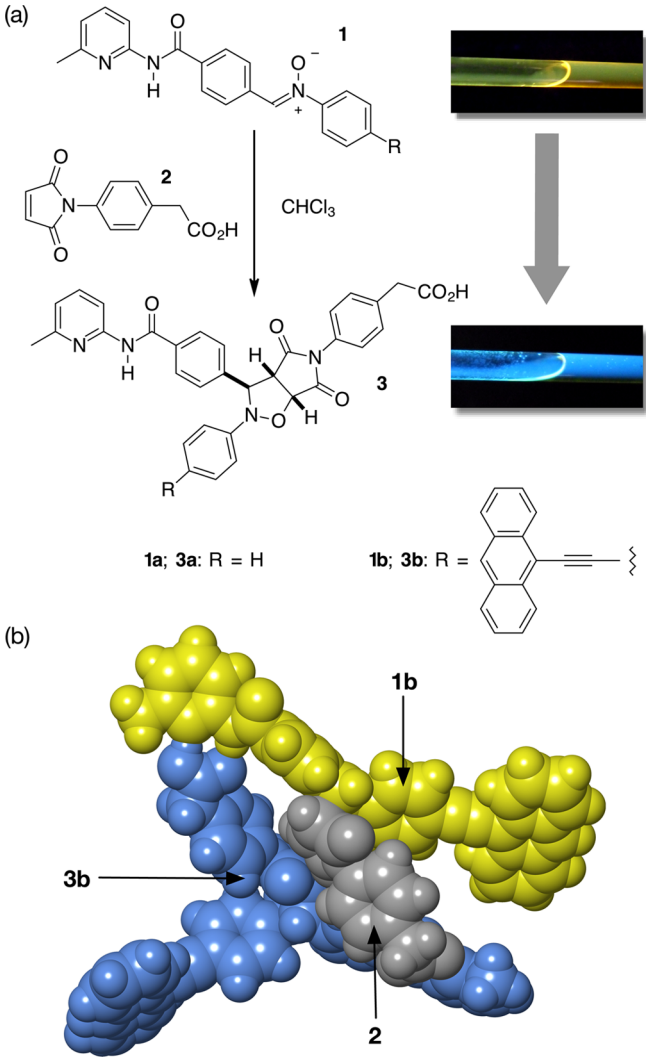

Figure 1. (a) Self-replicating template **3a** is constructed by the reaction of nitrone **1a** with maleimide **2** through the catalytically active [**1a**·**2**·**3a**] ternary complex. Replacement of the substituent R affords replicator **3b**, which incorporates a 9-ethynylanthracene optical tag, derived from nitrone **1b**. The formation of cycloadduct **3b**, mediated by ternary complex [**1b**·**2**·**3b**], is now associated with a change in fluorescence from yellow (**1b**) to blue (**3b**). (b) Calculated (RM1) structure of the transition state leading to **3b** from the ternary complex [**1b**·**2**·**3b**].

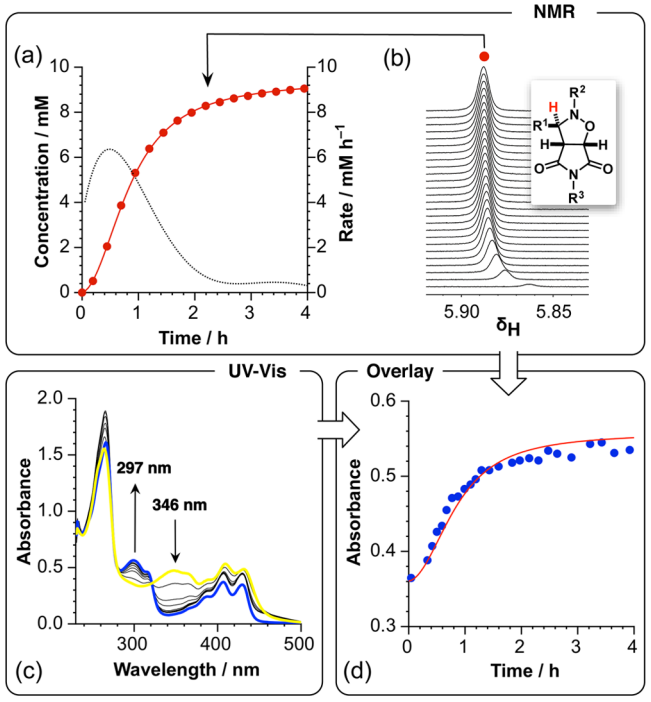

Figure 2. (a) Concentration (red circles) and rate (black dotted line) vs time profile for the formation of **3b** from nitrone **1b** and maleimide **2**, as determined by 500 MHz ^{1}H NMR spectroscopy ([**1b**] = [**2**] = 10 mM, 20 °C, $CDCl_3$). The red line shows the fit of the appropriate kinetic model to these data (see Supporting Information). (b) Appearance of the resonance associated with the formation of the *trans*-**3b** cycloadduct over time in the 500 MHz ^{1}H NMR spectrum of a reaction mixture containing **1b** and **2** ([**1b**] = [**2**] = 10 mM, 20 °C, $CDCl_3$). (c) Selected UV−vis spectra recorded during the reaction of **1b** and **2** ([**1b**] = [**2**] = 10 mM, 20 °C, $CDCl_3$), showing the disappearance of nitrone **1b** (346 nm band) and simultaneous appearance of cycloadduct **3b** (297 nm band). (d) Comparison of absorbance at 297 nm vs time. The blue circles show data determined experimentally from the spectra in panel c. The red line shows the absorbance at 297 nm computed using the concentrations of **3b** determined from the best fit of the appropriate kinetic model to the NMR data in panel a.

kinetic model are shown in Figure 2a,b. These kinetic experiments reveal that replicator **3b** is an excellent template for its own formation—the ternary complex [**1b**·**2**·**3b**] generates an effective molarity[13] (EM) of 16.2 M for the cycloaddition reaction (for details, see Supporting Information). This value for the ternary complex EM is broadly similar to those determined previously[9e,10b,11] for similar replicators and indicates that the incorporation of the 9-ethynylanthracene optical probe has essentially no effect on the functioning of the replicator.

Having established that **3b** was indeed capable of templating its own formation, we next sought to establish that the color change observed during this reaction is a signature of the autocatalytic replication processes. Accordingly, we monitored the formation of **3b** using UV−vis spectroscopy (Figure 2c) under conditions identical to those employed in the NMR kinetic experiments. As expected, the UV−vis spectra recorded during the reaction show the disappearance of a band corresponding to nitrone **1b** at 346 nm, with the concomitant appearance of a band at 297 nm corresponding to cycloadduct **3**. In order to relate these data to the kinetic data derived from NMR spectroscopy, we reconstructed the reaction profile at 297 nm by computing the expected absorbance at this wavelength from the concentrations of the components of the reaction mixture determined from the best fit our kinetic model to the NMR data. The excellent agreement (Figure 2d) between the calculated and observed reaction profiles provides compelling evidence that the color change observed during this reaction is indeed the signature of the replication of **3b**.

Normally, propagating reaction−diffusion fronts are observed in reactions that are initiated on flat plates or within capillary tubes. Since $CDCl_3$ is a relatively volatile solvent, we chose to investigate whether **3b** was capable of supporting a propagating reaction−diffusion front within a 50 μL gastight syringe of internal diameter 1.03 mm. Figure 3 illustrates our experimental setup. Two syringes were placed side-by-side in a specially constructed stand housed within a controlled environment where the temperature was regulated at 20 °C. One syringe was filled with a 5 mM solution of nitrone **1b** and

DOI: 10.1021/jacs.6b03372
J. Am. Chem. Soc. XXXX, XXX, XXX−XXX

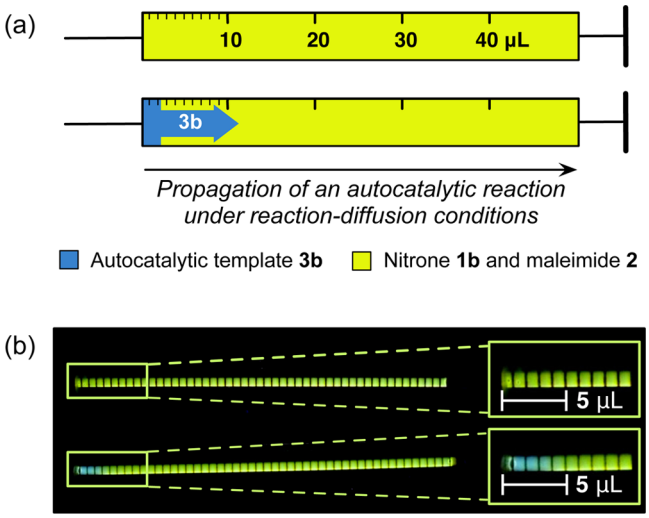

Figure 3. (a) Graphical representation and (b) photograph of the experimental setup employed for investigation of the propagating reaction–diffusion front initiated by replicator **3b** in two 50 μL gastight syringes. The upper syringe in each case represents the control experiment comprising the nitrone **1b** and maleimide **2** only ([**1b**] = [**2**] = 5 mM, 20 °C, $CDCl_3$). The lower syringe is seeded with ca. 2 μL of a solution of **3b** ([**1b**] = [**2**] = 5 mM, [**3b**] = 10 mM, 20 °C, $CDCl_3$).

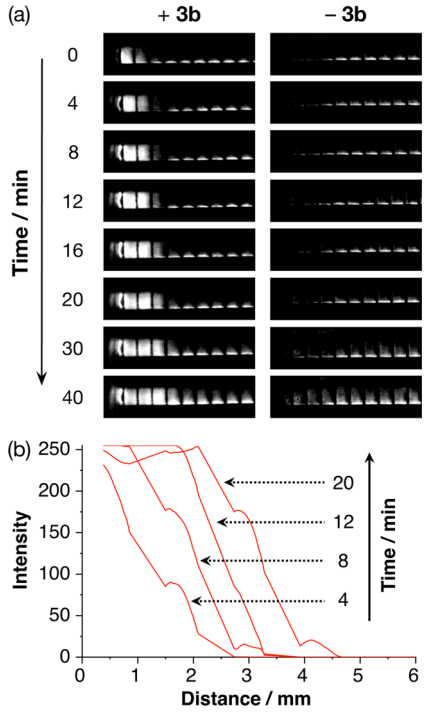

Figure 4. (a) Processed grayscale images, acquired over time, with the syringes illuminated using a 365 nm UV lamp, of the template-initiated reaction–diffusion experiment (+**3b**, left column) and the control experiment (−**3b**, right column). (b) Smoothed profiles of the grayscale images from the reaction–diffusion experiment (+**3b**) showing the progression of the reaction diffusion front over 20 min.

maleimide **2** in $CDCl_3$. The second syringe was prepared identically with the exception that approximately 2 μL of a 10 mM solution of replicator **3b** was drawn into the end of the syringe after it was filled with the solution of **1b** and **2**.

We envisaged that the syringe containing only **1b** and **2** would change color uniformly as replicator **3b** was formed. In the other syringe, the presence of **3b** would initiate the replication process, and the diffusion of the replicator thus formed would establish a reaction–diffusion front that would propagate along the syringe, being observed as the progression of a blue band along the initially yellow syringe.

The syringes were illuminated using a 365 nm UV lamp, and a color image was captured every 2 min using a digital camera. Processing of these images (see Supporting Information) afforded the data shown in Figure 4a. It is evident from these images that replicator **3b** has established (Figure 4a, +**3b**) a propagating reaction–diffusion front within the syringe to which it was added initially. By contrast, no such feature is evident within the control syringe (Figure 4a, −**3b**). As an additional control, we examined the diffusion of **3b** in the absence of an autocatalytic reaction. Approximately 2 μL of a 10 mM solution of replicator **3b** was drawn into the end of a syringe filled with a 5 mM solution of nitrone **1b** only in $CDCl_3$. In this case, the blue color of replicator **3b** disappears as a result of diffusion processes within the syringe, leaving the syringe visually indistinguishable from one that had been filled with nitrone **1b** only. No optical signature of a propagating reaction–diffusion front is observed in this case. Selected images were processed further (see Supporting Information) to compute the profile (Figure 4b) of the propagating front at a sequence of time points. These data clearly show the progression of the reaction–diffusion front mediated by replicator **3b** along the syringe. In many cases, reaction–diffusion fronts propagate at constant linear or radial velocity. However, in this case, the progression[14] of the front slows and will eventually stall as nitrone **1b** and maleimide **2** are depleted throughout the syringe as a result of the background rate of the cycloaddition reaction forming **3b** being significant on the time scale of the experiment.

Here, we have described the first example of a propagating reaction–diffusion front that is initiated and driven by a synthetic replicator. The work reported here represents a proof-of-principle. The successful implementation of a replicator-driven reaction–diffusion front, mediated by an autocatalytic replicator of defined structure and with specific interactions and catalytic relationships with other similar replicators, opens up[15] a number of exciting possibilities. This reaction format will allow us to explore networks[8a] of replicators under conditions and outcomes that lie far from the constraints[16] imposed by well-stirred batch reactors. These studies are currently underway in our laboratory.

■ ASSOCIATED CONTENT

Supporting Information

The Supporting Information is available free of charge on the ACS Publications website at DOI: 10.1021/jacs.6b03372. The research data supporting this publication can be accessed at http://dx.doi.org/10.17630/b05bac27-f50d-485b-966a-6b2246716481.

Experimental procedures, details of kinetic measurements and fitting, computational modeling of UV spectra, details of UV–vis and fluorescence analyses, and methods and analyses for the reaction–diffusion experiments (PDF)

DOI: 10.1021/jacs.6b03372
J. Am. Chem. Soc. XXXX, XXX, XXX–XXX

AUTHOR INFORMATION

Corresponding Author

*d.philp@st-andrews.ac.uk

Notes

The authors declare no competing financial interest.

ACKNOWLEDGMENTS

We thank EPSRC for postgraduate studentship awards to J.H. (EP/E017851/1) and T.K. (EP/K503162/1).

REFERENCES

(1) (a) Jee, E.; Bánsági, T., Jr.; Taylor, A. F.; Pojman, J. A. *Angew. Chem., Int. Ed.* **2016**, *55*, 2127. (b) Showalter, K.; Epstein, I. R. *Chaos* **2015**, *25*, 097613. (c) Vanag, V. K.; Epstein, I. R. *Int. J. Dev. Biol.* **2009**, *53*, 673. (d) Vanag, V. K.; Epstein, I. R. *Chaos* **2008**, *18*, 026107. (e) Epstein, I. R.; Pojman, J. A.; Steinbock, O. *Chaos* **2006**, *16*, 037101. (f) Mikhailov, A. S.; Showalter, K. *Phys. Rep.* **2006**, *425*, 79. (g) Taylor, A. F.; Britton, M. M. *Chaos* **2006**, *16*, 037103. (h) Johnson, B. R.; Scott, S. K. *Chem. Soc. Rev.* **1996**, *25*, 265. (i) Pojman, J. A. Frontal Polymerization. In *Polymer Science: A Comprehensive Reference*; Matyjaszewski, K., Möhler, M., Eds.; Elsevier B.V.: Amsterdam, 2012; pp 3018−3020.

(2) (a) Kondo, S.; Miura, T. *Science* **2010**, *329*, 1616. (b) Volpert, V.; Petrovskii, S. *Phys. Life Rev.* **2009**, *6*, 267. (c) Camazine, S.; Deneubourg, J.-L.; Franks, N. R.; Sneyd, J.; Theraulaz, G.; Bonabeau, E. Self-Organization in Biological Systems. In *Princeton studies in complexity*; Anderson, P. W., Epstein, J. M., Foley, D. K., Levin, S. A., Nowak, M. A., Eds.; Princeton University Press: Princeton, NJ, 2003. (d) Hess, B. *Naturwissenschaften* **2000**, *87*, 199. (e) Ball, P. *The Self-made Tapestry: Pattern Formation in Nature*; Oxford University Press Inc.: New York, 2001.

(3) (a) *Chemical waves and patterns*; Kapral, R., Showalter, K., Eds.; Kluwer Academic Publishers: Berlin, 2012. (b) Grzybowski, B. A. *Chemistry in Motion*; John Wiley & Sons, Ltd.: New York, 2009. (c) Epstein, I. R.; Pojman, J. A. *An introduction to nonlinear chemical dynamics: oscillations, waves, patterns, and chaos*; Oxford University Press: Oxford, UK, 1998. (d) Cross, M. C.; Hohenberg, P. C. *Rev. Mod. Phys.* **1993**, *65*, 851.

(4) Boga, E.; Peintler, G.; Nagypál, I. *J. Am. Chem. Soc.* **1990**, *112*, 151.

(5) (a) McCaskill, J. S.; Bauer, G. J. *Proc. Natl. Acad. Sci. U. S. A.* **1993**, *90*, 4191. (b) Bauer, G. J.; McCaskill, J. S.; Otten, H. *Proc. Natl. Acad. Sci. U. S. A.* **1989**, *86*, 7937.

(6) (a) Zadorin, A. S.; Rondelez, Y.; Galas, J. C.; Estévez-Torres, A. *Phys. Rev. Lett.* **2015**, *114*, 068301. (b) Padirac, A.; Fujii, T.; Estévez-Torres, A.; Rondelez, Y. *J. Am. Chem. Soc.* **2013**, *135*, 14586.

(7) (a) Bissette, A. J.; Fletcher, S. P. *Angew. Chem., Int. Ed.* **2013**, *52*, 12800. (b) Huck, J.; Philp, D. *Supramolecular Chemistry: From Molecules to Nanomaterials*; John Wiley & Sons, Ltd.: New York, 2012; Vol. *4*, pp 1415−1446. (c) Plasson, R.; Brandenburg, A.; Jullien, L.; Bersini, H. *Artif. Life* **2011**, *17*, 219. (d) Vidonne, A.; Philp, D. *Eur. J. Org. Chem.* **2009**, *2009*, 593. (e) Patzke, V.; von Kiedrowski, G. *ARKIVOC* **2007**, *46*, 293. (f) Paul, N.; Joyce, G. F. *Curr. Opin. Chem. Biol.* **2004**, *8*, 634.

(8) (a) Kassianidis, E.; Pearson, R. J.; Wood, E. A.; Philp, D. *Faraday Discuss.* **2010**, *145*, 235. (b) Ashkenasy, G.; Ghadiri, M. R. *J. Am. Chem. Soc.* **2004**, *126*, 11140. (c) Yao, S.; Ghosh, I.; Zutshi, R.; Chmielewski, J. *Nature* **1998**, *396*, 447. (d) Sievers, D.; von Kiedrowski, G. *Chem. - Eur. J.* **1998**, *4*, 629.

(9) (a) Dadon, Z.; Samiappan, M.; Wagner, N.; Ashkenasy, G. *Chem. Commun.* **2012**, *48*, 1419. (b) Carnall, J. M. A.; Waudby, C. A.; Belenguer, A. M.; Stuart, M. C. A.; Peyralans, J. J.-P.; Otto, S. *Science* **2010**, *327*, 1502. (c) Nguyen, R.; Allouche, L.; Buhler, E.; Giuseppone, N. *Angew. Chem., Int. Ed.* **2009**, *48*, 1093. (d) Xu, S.; Giuseppone, N. *J. Am. Chem. Soc.* **2008**, *130*, 1826. (e) Sadownik, J. W.; Philp, D. *Angew. Chem., Int. Ed.* **2008**, *47*, 9965.

(10) (a) Vidonne, A.; Kosikova, T.; Philp, D. *Chem. Sci.* **2016**, *7*, 2592. (b) Kosikova, T.; Hassan, N. I.; Cordes, D. B.; Slawin, A. M. Z.; Philp, D. *J. Am. Chem. Soc.* **2015**, *137*, 16074. (c) Vidonne, A.; Philp, D. *Tetrahedron* **2008**, *64*, 8464.

(11) Kassianidis, E.; Philp, D. *Angew. Chem., Int. Ed.* **2006**, *45*, 6344.

(12) For an example of an optical readout amplified by autocatalysis, see: Mohapatra, H.; Schmid, K. M.; Phillips, S. T. *Chem. Commun.* **2012**, *48*, 3018.

(13) (a) Page, M. I.; Jencks, W. P. *Proc. Natl. Acad. Sci. U. S. A.* **1971**, *68*, 1678. (b) Page, M. I. *Chem. Soc. Rev.* **1973**, *2*, 295. (c) Kirby, A. J. *Adv. Phys. Org. Chem.* **1980**, *17*, 183.

(14) In certain cases, convection can affect wave front propagation. For a discussion of convective effects on chemical waves, see: Pojman, J. A.; Epstein, I. R. *J. Phys. Chem.* **1990**, *94*, 4966.

(15) Merkin, J. H.; Poole, A. J.; Scott, S. K.; Masere, J.; Showalter, K. *J. Chem. Soc., Faraday Trans.* **1998**, *94*, 53.

(16) (a) Kosikova, T.; Mackenzie, H.; Philp, D. *Chem. - Eur. J.* **2016**, *22*, 1831. (b) Sadownik, J.; Philp, D. *Org. Biomol. Chem.* **2015**, *13*, 10392.

DOI: 10.1021/jacs.6b03372
J. Am. Chem. Soc. XXXX, XXX, XXX−XXX